Ground-based telescopic observations of Jupiter's aurora at visible wavelength

Yohei Harayama

Physics of Earth and Planetary Atmosphere Group,
Division of Earth and Planetary Science, Hokkaido University

25 March 2002

Abstract

Jupiter's auroral emissions have been observed by spacecrafts and Hubble Space Telescope in space. However, it is difficult to observe continuously the emissions and the variations in time. It is important to note that the Jupiter's aurora contains the emission of the first Balmer line of atomic hydrogen, Hα(656.3 nm). It is generally believed that the ground-based observation of emissions in visible wavelength is difficult because of the strong reflection of sunlight on Jupiter's surface.

We have built an observational system with a CCD camera and a narrow band pass filter in Hα wavelength. We observed Jupiter by using 115-cm telescope at Ginganomori Observatory, Hokkaido, and 60-cm telescope at the Iitate Observatory, Fukushima in Japan from November 1999 to November 2001.

We analyzed the data acquired on October 29 - November 1, 2001 because the atmosphere of Earth was relatively steady for ground-based observation. We made a composite image from short exposure images to reduce the influence of Earth's atmospheric turbulence. Using this technique, we detected a faint emission at Hα wavelength in Jupiter's northern auroral region by subtracting the background image at neighbor wavelength from the Hα image. The ratio of the faint emission to background intensity is $\sim$1.3 %. Our technique may be applied to other observations such as faint emissions on planetary atmosphere and faint luminous bodies.

Contents

1 Introduction **1**
1.1 Jupiter's Aurora . . . 1
1.2 Previous observations of Jupiter's aurora . . . 1
1.2.1 UV observations . . . 1
1.2.2 IR observations . . . 3
1.2.3 Visible observations . . . 4
1.3 Purpose of this study . . . 5

2 Instrument **6**
2.1 Optics . . . 6
2.1.1 Interference filter . . . 6
2.1.2 CCD camera . . . 9
2.1.3 Telescope . . . 10
2.2 Fringes . . . 12
2.3 Estimation of the Jupiter's visible aurora . . . 13
2.3.1 Intensity and width of auroral oval . . . 13
2.3.2 Intensity of Background emission . . . 14
2.3.3 Signal to Noise ratio . . . 14

3 Observations **15**
3.1 Observation Period and Site . . . 15
3.2 Procedure for observation . . . 17
3.2.1 Setup of the imaging system . . . 17
3.2.2 Imaging . . . 17

4 Data Processing **19**
4.1 Method . . . 19
4.2 Image Processing . . . 19

5 Results and Discussion **21**
5.1 Results . . . 21
5.2 Discussion . . . 27

6 Summary **29**

1 Introduction

1.1 Jupiter's Aurora

Jupiter has a large magnetosphere because Jupiter has a very strong magnetic field, which is 50000 times as strong as Earth's one. Therefore, there are auroral emissions observed in X-ray, UV, visible, Infrared, and radio wavelength ranges on Jupiter's atmosphere. Jupiter's auroral emissions are mainly generated through the excitation of upper atmospheric atoms and molecules of hydrogen by energetic electrons and ions precipitating down from the magnetosphere along high-latitude magnetic field lines. Most of the UV emissions are thought to be due to H Lyα (121.6 nm) and H_2 Lyman and Werner band. The visible emissions are due to the Balmer series of H, mainly Hα (656.3 nm). There are emissions by H_3^+ (2 - 4 μm) at IR wavelengths. H_3^+ is formed in the middle ionosphere by following reaction:

$$H_2 + e \rightarrow H_2^+ + 2e$$

$$H_2 + H_2^+ \rightarrow H_3^+ + H$$

In the present study, we select the Hα emission to observe Jupiter's visible aurora. The equation of line spectrum found out by Balmer is

$$\frac{1}{\lambda} = R(\frac{1}{2}^2 - \frac{1}{n}^2)$$

$$n = 3, 4, 5 \cdots$$

where R is the Rydberg constant. Hα is the emission of $n = 3$ in this equation.

Spatial distributions of auroral emissions are thought to be almost same in all wavelengths. One of auroral regions is main oval that are located around the magnetic poles and corotates with the planet, in contrast with the Earth's auroral pattern. The magnetic dipole of Jupiter is tiltes at $\sim$10° to the rotation axis. Because the equatormost part of the northern main oval is located at $\sim$170° W in System-III longitude, we can observe it from Earth at $\sim$170° central meridian longitudes (CML). The main oval may not be influenced by solar wind. Second auroral region is polar cap emission that is diffuse emission inside the main oval and associated with the outer magnetosphere. Third auroral region is Io footprint that is associated with the magnetic footprint of Io's orbit at 5.9 R_J. The Io footprint may be generated by the precipitation of oxygen and sulfur that erupted by the volcanic activities on Io.

1.2 Previous observations of Jupiter's aurora

1.2.1 UV observations

The first positive identification of the Jupiter's aurora was provided by the Voyager ultraviolet spectrometer (UVS). The UVS observations inferred H Lyα (121.6 nm) and H_2 Lyman and Werner band emissions. UV aurora has been observed by the Galileo spacecraft's UVS and Extreme ultraviolet spectrometer (EUVS), and Hubble space telescope (HST) Wide-Field Planetary Camera 2 (WFPC2). *Waite et al.* (2001) reported that the Hubble Space Telescope Imaging

Spectrogragh (STIS) observed a flare of auroral emission located poleward of the northern main oval (Fig 1). The intensity of the emission increased by a factor of 30 within 70 s. The region of emission is connected magnetically to outer magnetosphere, and the flare may be related directly to changes in the solar wind.

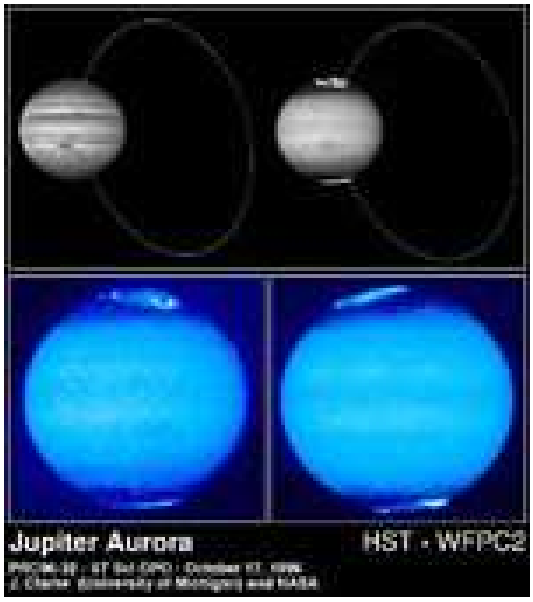

Figure 1: UV aurora observed by HST's WFPC2 [http://www.jpl.nasa.gov/galileo/].

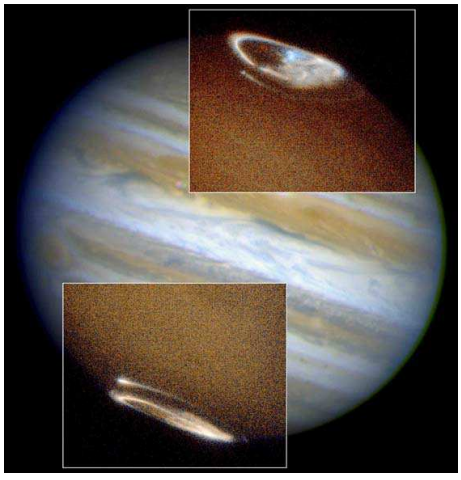

Figure 2: False-color image of UV aurora observed by HST's STIS [http://oposite.stsci.edu/pubinfo/1998.html].

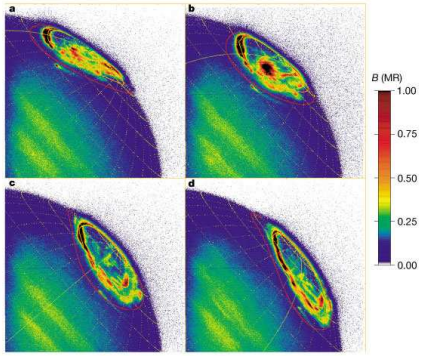

Figure 3: Auroral flare observed by HST's STIS [*Waite et al.*, 2001].

1.2.2 IR observations

Jupiter's IR aurora has been observed by ground-based telescopes since 1980's at wavelengths in the range 2 - 8 μm, where reflected sunlight is absorbed strongly by methane and ammonia.

In Jupiter's magnetosphere, the H_3^+ ion, probably of ionospheric origin, was detected by the Voyager's UVS. The Canada-France-Hawaii telescope (CFHT) detected H_3^+ first in the southern auroral region of Jupiter [*Drossart et al.,* 1989]. The ProtoCAM infrared camera at the 3 m telescope of the Infrared Telescope Facility (IRTF) observed 3 - 4 μm emissions of thermally excited H_3^+ ions in the upper atmosphere. H_3^+ emissions have been observed by NSFCAM at IRTF, and the distribution of the emissions is interpreted by magnetic field model [*Satoh and Connerney,* 1999]. The most intense emissions are found between the 12 - 30 R_J ovals, representing the main auroral emission.

Observations of Jupiter's IR aurora are not only at IRTF but also in other observatories. On July 22 - 24, 1994, *Mai and Jockers* (2000) observed full disk images of Jupiter's H_3^+ and H_2 emission at 2.093 and 2.121 μm by the IRAC-2b near-infrared camera with Fabry-Perot-interferometer at the 2.2 m telescope of the European Southern Observatory (ESO) in Chile. Infrared Spectrometer And Array Camera (ISAAC) at Very Large Telescope (VLT) obtained H_3^+ emissions at 2-4 μm in November 2000 (Fig 5).

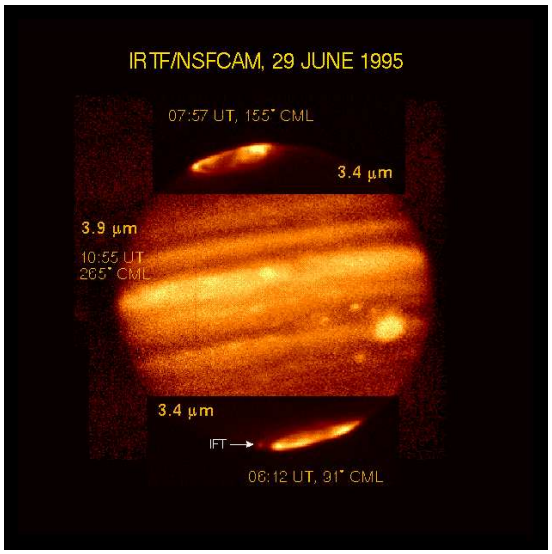

Figure 4: IR aurora observed by IRTF [*T. Satoh and J. E. P. Connerney,* 1999].

Figure 5: IR aurora observed by VLT at ESO[http://www.eso.org/outreach/press-rel/].

1.2.3 Visible observations

Jupiter's visible aurora is mainly observed by Galileo spacecraft. As early observations, *Hunter et al.* (1969) observed Hα activity on Jupiter by using 16-inch telescope in the 1960s, and 26-inch telescope at the University of South Florida in the 1970s [*Clary and Hunter* (1975) and *Holman and Hunter* (1977)]. These observations suggested the existence of visible aurora, but they were ambiguous. Voyager spacecraft observed Jupiter's dark side in 1979. *Cook et al.* (1981) concluded that at the imaging experiment was most probably auroral emission caused by particle precipitation from the Io torus. The total emission rate in the wavelength range 400 - 600 nm was estimated to be $\sim$5 kR (an estimated factor of 4 limb enhancement combined with an observed slant intensity of about 20 kR). Recently, Galileo spacecraft's Solid State Imaging (SSI) camera observed northern visible aurora on Jupiter's nightside. *Ingersoll et al.* (1998) estimated that the total intensity of emission was $\sim$80 - $\sim$300 kR, the full width of the oval varied from under 500 km to over 8000km, and the particles that cause the aurora originate on Jupiter's equatorial plane $\sim$13 R_J from the center of the planet. *Vasavada et al.* (1999) observed four classes of emission: primary arc, secondary arc, "polar cap" emission and Io footprint. They estimated that the full width at half maximum (FWHM) of the primary arc was 170 - 460 km. The tipical intensity was $\sim$1.3 MR and brightest emission was $\sim$6.6 MR.

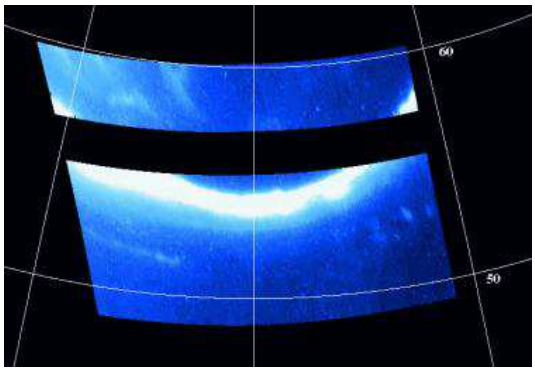

Figure 6: The equatomost part of the northern aurora oval on Jupiter's nightside [*Ingersoll et al.*, 1998].

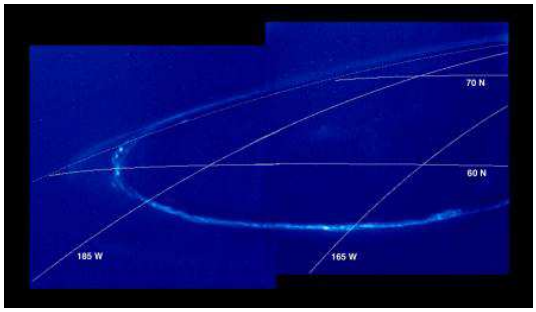

Figure 7: Limb-brightened "polar cap" emission is visible along the limb [*Vasavada et al.*, 1999].

1.3 Purpose of this study

Jupiter's aurora have been observed by spacecrafts, Hubble Space Telescope and ground-based telescopes at various wavelengths. However, Galileo spacecraft observed aurora only a several times at visible wavelength. It is difficult to observe continuously the emissions and the variations in time by using spacecrafts. It is generally believed that ground-based observation of emissions in visible wavelength is difficult because of strong reflection of sunlight on Jupiter's surface. Therefore we tried to build a technique of ground-based observation at visible wavelength to understand the emission mechanism on Jupiter's aurora.

Auroras are high-latitude atmospheric emissions that result from the precipitation of energetic charged particles from planetary magnetosphere. Studying Jupiter's magnetosphere, through observations of Jupiter's auroral phenomena, will provide useful information to study planetary magnetosphere and related research areas.

2 Instrument

2.1 Optics

Our Imaging system is composed of telescope, slit, collimator lens, narrow band interference filter, focusing lens, and CCD camera as a detector (Fig 8). The focal length of two lenses is different at each telescope. The imaging system can target other objects at various wavelengths by replacing filter.

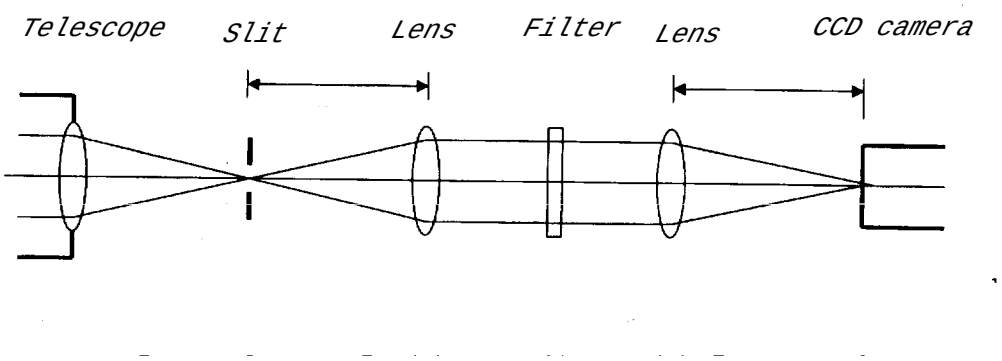

Figure 8: Schematic diagram of imaging system.

2.1.1 Interference filter

We have been observed Jupiter's aurora at Hα wavelength. For observation of the Hα emission, we prepared 4 narrow band filters. Full Width at Half Maximum (FWHM) are 0.12, 0.15, 0.33 and 1.55 nm. Transmission functions of these filters are shown in Fig 9, 10, 11, 12. In the present thesis, we show results of data obtained by using FWHM 0.15 and 1.55 nm filters mainly. For other observations such as cloud patterns of Jupiter and Venus, we prepared several filters at various wavelengths.

Figure 9: Transmission function of FWHM 0.12 nm filter.

Figure 10: Transmission function of FWHM 0.15 nm filter.

Figure 11: Transmission function of FWHM 0.33 nm filter.

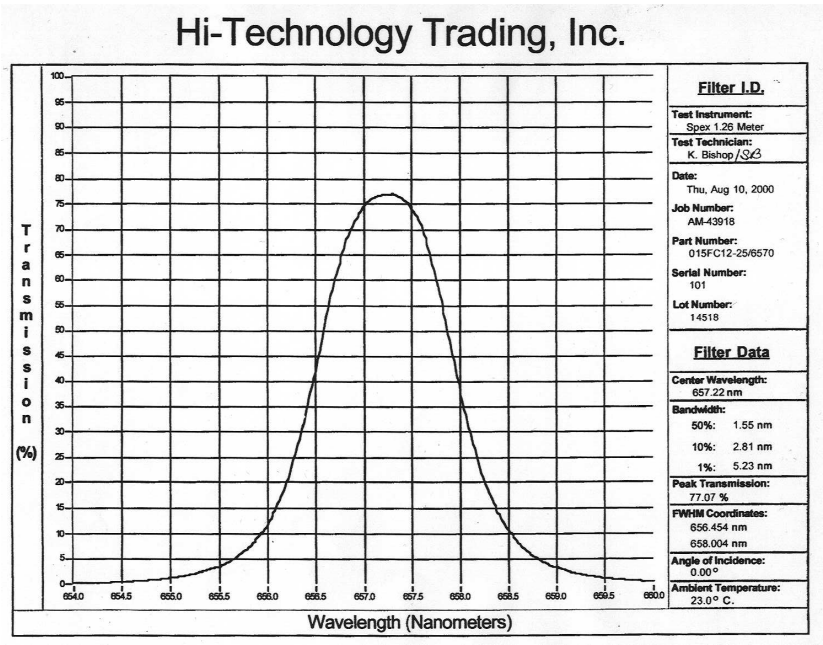

Figure 12: Transmission function of FWHM 1.55 nm filter.

2.1.2 CCD camera

CCD cameras that we have been used are SpectraVideo and PlutoCCD manufactured by PixelVision, Inc. These CCD cameras have high quantum efficiency because they are available back-illuminated. Dark current noise is low because of thermoelectric cooling. We can obtain several images in a second by PlutoCCD which has a high frame rate performance. Characteristics of CCD cameras are as follows:

- SpectraVideo
  - Imaging Resolution: 512 $\times$ 512 pixels
  - Pixel Size: 24 μm $\times$ 24 μm
  - Gain: Low/High: 8.61/1.85 (electrons/DN)
  - Read out Noise: Typical 7 (electrons at 50 k pix/sec)
  - Dark Current: 1 (electron/pixel/sec at - 45 °C)
  - Cooling Capacity: -45 to -55 (°C from ambient)
  - Digitization: 16 bits
- PlutoCCD
  - Imaging Resolution: 625 $\times$ 488 pixels
  - Pixel Size: 12 μm $\times$ 12 μm
  - Gain: Low/High: Typical 4.5/1.2 (electrons/DN)
  - Read out Noise: Lo/High: 25/30 (electrons RMS)
  - Dark Current: 20 (electron/pixel/frame at - 5 °C)
  - Cooling Capacity: -40 (°C from ambient)
  - Digitization: 14 bits

2.1.3 Telescope

We have observed Jupiter by using the Rikubetsu 115-cm telescope at Ginganomori Observatory, Hokkaido (Fig 13), and the Iitate 60-cm telescope at the Iitate Observatory, Fukushima (Fig 15) in Japan. We used 10-cm telescope additionally to test imaging at Hokkaido University, Sapporo (Fig 17). Imaging sensor composed of optics and CCD camera was mounted at the Nasmyth focus of the Rikubetsu telescope (Fig 14) and at Coude focus of the Iitate telescope (Fig 16). Characteristics of telescopes are as follows:

- Rikubetsu 115-cm telescope
  - Effective Diameter: 110 cm
  - Focal Length: 8800 mmiNasmyth focusj
- Iitate 60-cm telescope
  - Effective Diameter: 60 cm
  - Focal Length: 14400 mmiCoude focusj
- 10-cm
  - Effective Diameter: 105 mm
  - Focal Length: 820 mm

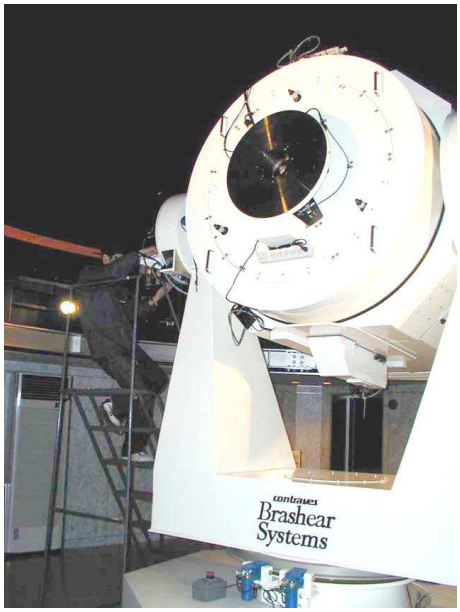

Figure 13: Rikubetsu 115-cm telescope.

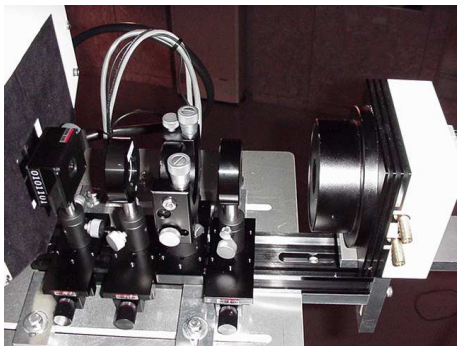

Figure 14: Imaging sensor mounted at the Nasmyth focus.

Figure 15: Iitate 60-cm telescope.

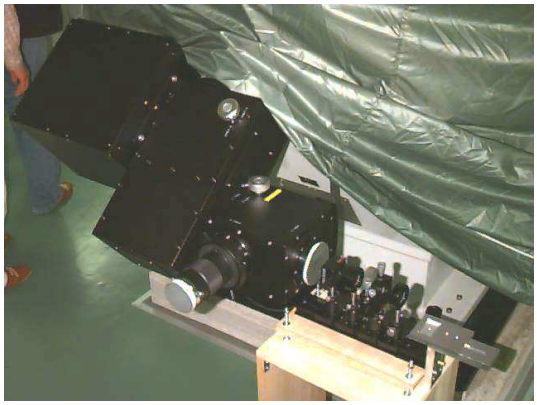

Figure 16: Image sensor mounted at the Coude focus.

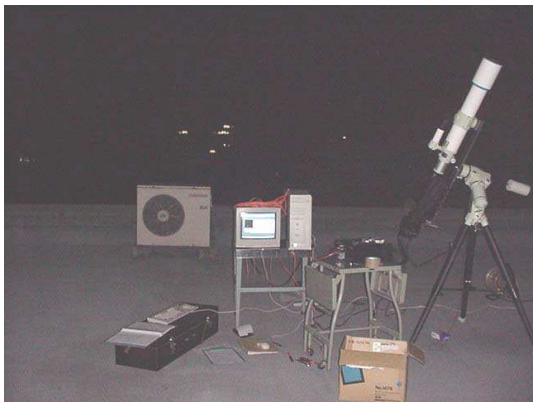

Figure 17: View of test observation with 10-cm telescope.

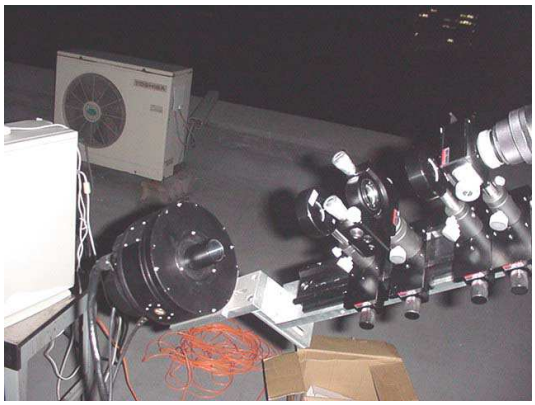

Figure 18: Image sensor mounted at the 10-cm telescope.

2.2 Fringes

A transmission function of interference filter is generally dependent on temperature and incident angle of the light. When a temperature decreases, the center wavelength of filter is shifted to a short wavelength. Coefficients of temperature of filters we used were ∼0.02 nm/°C. When the incident angle of light is θ, the transmitted wavelength λ is given by

$$\lambda = \lambda_0 \sqrt{1 - \left(\frac{1}{n}\right)^2 \sin^2\theta}$$

where λ_0 is wavelength of light, n is refractive index. Therefore, a light with an incident angle goes through a narrow band filter and makes an interference fringe on CCD's chip. When we observe an emission, we have to know where the emission focuses on CCD's chip through the filter. For observation of the Hα emission, we obtain images of fringe in order to see the region of the emission by using Hα lamp (Fig 19). When we observe Jupiter, we put the Jupiter's auroral region in the fringe in order to detect the emission at Hα wavelength. Images of fringe obtained by FWHM 0.15, 1.55 nm filter are shown in Fig 20, 21).

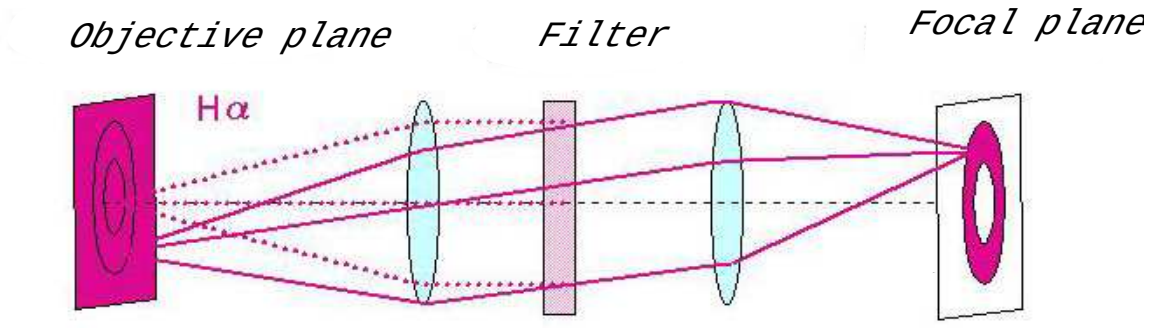

Figure 19: Imaging a fringe of Hα emission. We illuminate the screen placed at the focal plane of telescope by Hα lamp. Hα emission with an incident angle pass the filter and make a fringe on CCD.

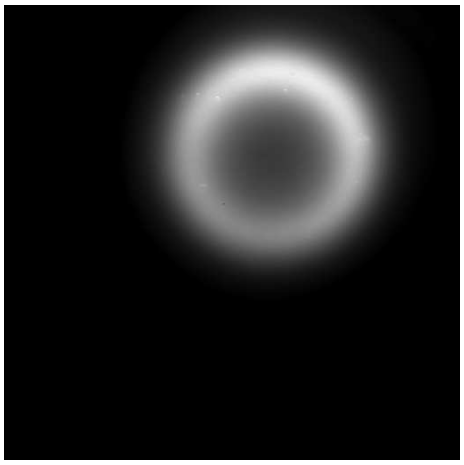

Figure 20: Image of fringe obtained by FWHM 0.15 nm filter.

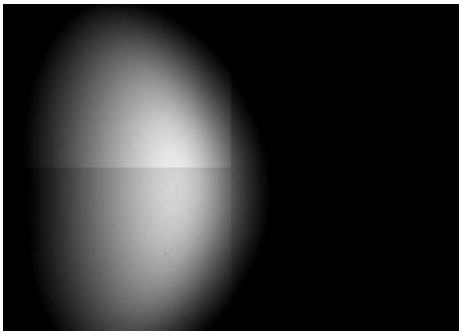

Figure 21: Image of fringe obtained by FWHM 1.5 nm filter.

2.3 Estimation of the Jupiter's visible aurora

The estimation of the Jupiter's visible aurora of ground-based observation is shown in this section. To represent the intensity of aurora, the Rayleigh (R) unit is commonly used. The photometric definition of (R) is as follows:

- If the radiance from a certain direction is measured as I [$photons \cdot cm^2 \cdot sterad^{-1} \cdot s^{-1}$], the radiance intensity is defined as 4πI/10^6 *Rayleighs*;

$$1R = \frac{10^6}{4\pi} photons \cdot cm^2 \cdot sterad^{-1} \cdot s^{-1}$$

2.3.1 Intensity and width of auroral oval

Ingersoll et al. (1998) reported that the intensity of northern auroral emission varied from $\sim$80 to $\sim$300 kR. When the total intensity in the clear filter (385 - 935 nm) image was 80 kR, the intensity in the red filter (625 - 705 nm) image was $\sim$30 kR. The emission in the red filter image was mainly do to Hα emission. Therefore, more than 30 % of the total intensity was due to Hα emission. In this case, we can estimate that the Hα emission was estimated in the range of $\sim$30 - $\sim$90 kR. *Vasavada et al.* (1999) estimated that the tipical intensity of the primary arc was typically $\sim$1.3 MR and the brightest emission was $\sim$6.6 MR. In this case, we can estimate that Hα emission was typically $\sim$400 kR and the brightest emission was $\sim$2 MR. In addition, in UV observation, the Hubble Space Telescope Imaging Spectrograph (STIS) observed a flare of auroral emission and the intensity of the emission increased by a factor of 30 within 70 s. Probably, there is such flare also in visible emissions. Therefore, we estimate that the intensity of Hα emission is $\sim$100 kR - $\sim$1 MR. *Ingersoll et al.* estimated that the full width of the oval was from under 500 km to over 8000 km. While, *Vasavada et al.* estimated that the full width

at half maximum (FWHM) of the primary arc was 170 - 460 km. Therefore, we estimate that the full width of the oval is ∼1000 km typically.

2.3.2 Intensity of Background emission

When we observe Jupiter from the vicinity of the Earth, the strong reflection of sunlight on Jupiter's surface is observed as background emission. It is thought that the intensity of continuum emission from Jupiter's surface is ∼5 MR/0.1 nm. However, Hα emission is a absorption line known as Fraunhofer line and there is some limb darkening at the auroral region on disk of Jupiter. Therefore, we estimate that the background emission at Hα (656.3 nm) is ∼500 kR/0.1 nm. When we use FWHM 0.15 nm filter and 1.55 nm filter, the background emission are estimated ∼750 kR, ∼ 7.75 MR respectively.

2.3.3 Signal to Noise ratio

The theoretical spatial resolution of our imaging system is ∼0.3 "/pixel corresponding to ∼1000 km/pixel on Jupiter's surface. The practical resolution is ∼4000 km/4 pixels because the limiting resolution of ground-based observation is ∼1 " at the best. Assuming the intensity of the auroral oval is 400 kR and the width is 1000 km, the intensity of auroral oval of image would be ∼100 kR and the width would be diffused over several pixels. In the image obtained by 1.55 nm filter, the ratio of the auroral emission to the background emission is ∼1.3 %. Since we detect the Hα emission by subtracting the background image of Jupiter from the Hα image by image processing, we have to compare the auroral emission with the fluctuation of the backgound emission. In a image obtained by CCD camera, the fluctuation of the N counts emission is generally represented as $\pm\sqrt{N}$. When we make a composite image from short exposure images, the ratio of the auroral emission to $\pm\sqrt{N}$ would increase. We estimate that the Hα emission is detectable in the composite image of more than 10 s integration time in the case of Iitate observation.

3 Observations

3.1 Observation Period and Site

We can observe Jupiter for 3 - 4 months a year since Jupiter is an outer planet. The time near the Jupiter's opposition is more suitable for observation. When we plan the observation of Jupiter, we have to consider the condition of Earth's atmosphere. For example, the condition is not good in midwinter in Japan because of the wind. Imaging observations of Jupiter by Rikkubetsu telescope, Iitate telescope and 10-cm telescope were carried out during the period from November 1999 to November 2001. In the first season in 1999, we had test observations by using Rikubetsu telescope and Iitate telescope. In the second season in 2000, we obtained the Hα images and the Background images by using a Hα lamp in order to detect a faint auroral emission by image processing. In the third season in 2001, we obtained a lot of dataset and some of them are obtaioned in good seeing conditions. The schedule of observations is given in Table 1.

Date	Sites	Filter	Notes
The first season			
1999.11.28 ~ 11.30	Rikubetsu	Hα(0.33 nm) Hα(0.15 nm) Others	We tested the imaging system and obtained images by many filters.
1999.12.26 ~ 12.28	Iitate	Hα(0.15 nm) Hα(0.33 nm)	We tested the imaging system and the Hα lamp.
2000.2.27	Iitate	Hα(0.15 nm)	We obtained a large number of dataset.
The second season			
2000.8.27 ~ 9.5	Rikubetsu	Hα(0.15 nm)	We used a spare CCD camera because of the trouble of the main camera.
2000.10.21 2000.11.4	Sapporo	Hα(0.15 nm)	We observed by 10-cm telescope and obtained a large number of dataset.
2000.12.4 ~ 12.11	Rikubetsu	Hα(0.15 nm)	We obtained a large number of dataset. The seeing was an average.
The third season			
2001.10.3 ~ 10.9	Rikubetsu	Hα(0.15 nm)	
2001.10.15 ~ 10.18	Rikubetsu	Hα(0.15 nm)	The seeing was good.
2001.10.23 ~ 10.26	Iitate	Hα(1.55 nm)	The seeing was an average. We obtained a large number of dataset.
2001.10.29 ~ 11.1	Iitate	Hα(1.55 nm) Hα(0.12 nm)	The seeing was very good.

Table 1: Schedule of observations.

3.2 Procedure for observation

3.2.1 Setup of the imaging system

The Imaging system can be used with three telescopes by changing lenses. We put the imaging system on the telescope and operate the CCD camera by a PC. The most important thing in setup of the imaging system is the adjustment of focus. The procedure for the adjustment of focus is as follows:

1. We put two lenses and the CCD camera on the optical rail and guide the optical axis to the CCD camera.
2. We remove the focusing lens and put a screen near the focal plane of telescope. We adjust the focus of the collimator lens by hand through the CCD monitor.
3. We put the focusing lens and adjust the focus by hand through the monitor.
4. We remove the screen and adjust the focus of telescope.

We note the lengths between the screen(focal plane of telescope) and the collimator lens, and between the focusing lens and the CCD camera for next time.

3.2.2 Imaging

The procedure for imaging is mainly three steps as follows:

1. Fringe
   We obtain a fringe by using Hα lamp in order to see the region of the fringe on CCD's chip.
2. Hα image
   We guide Jupiter's auroral regions to the region of fringe and take the image. We call this image Hα image. The Hα image is obtained at Hα wavelength, so it contains the Hα emission of the auroral oval. We obtain $\sim$100 - 200 frames at a time.
3. Background image (Offline image)
   We displace Jupiter's auroral regions from the region of fringe and take the image. We call this image Background (BG) image. The BG image is obtained at neighbor wavelength, so it does not contain the Hα emission of the auroral oval. We obtain $\sim$100 - 200 frames at a time.

We took a few minutes to obtain a cycle of images. We repeated this cycle at different exposure time. The range of exposure time was from 25 ms to 500 ms. Furthermore, we obtained dark frames in this cycle. Illustration of imaging Hα and BG images is shown in Fig 22.

When we observe Jupiter's aurora, we have to know the Central meridian longitudes (CML). Jupiter's northern auroral oval corotates with the planet and the equatormost part of the oval is located at $\sim$170° W in System - III longitude (Fig 23). Therefore, we targeted the northern auroral region during CML 80° - 260° and the southern auroral region in other time.

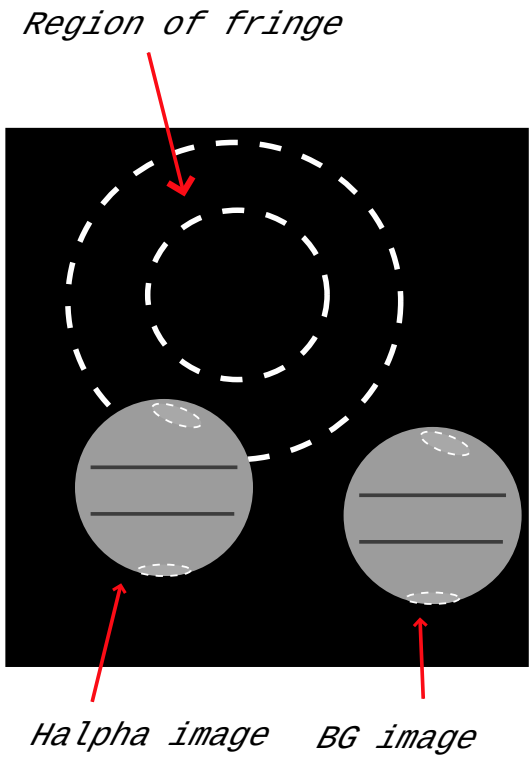

Figure 22: Illustration of imaging a Hα image and a BG image. The northern auroral region are guided to the region of fringe.

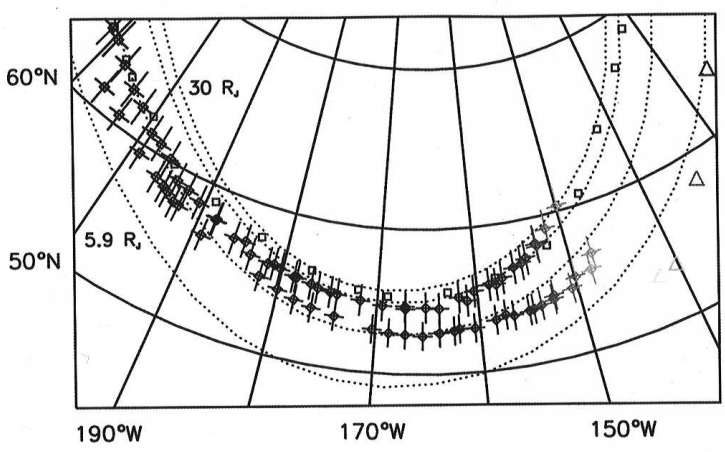

Figure 23: The map of the northern auroral oval. [Vasavada et al.,1999]

4 Data Processing

4.1 Method

The first step of this study is to obtain the intensity and distribution of the Hα emission. We have tried three ways in order to detect a Hα emission.

1. We compare profiles of Jupiter's auroral regions in a Hα image and a BG image.
2. We obtain a image by subtracting a BG image from a Hα image, and see the profile of auroral regions.
3. We make composite images from short exposure images before subtraction.

4.2 Image Processing

The image processing procedure is as follows:

1. Making of composite images
   We make a composite Hα image from 10 - 200 Hα images obtained with short exposure time. Hα images are not fully aligned because of shift and distorsion of the images caused by Earth's atmosphere. Therefore, we have to align them in order to making a composite image in this process. We divide the intensity of the composite image by the number of frames. We make a composite BG image in the same way.
2. Matching of composite images
   We calculate the displacement between the BG image and the Hα image for matching of disks.
3. Subtraction
   We make a image by subtracting the BG image from the Hα image. In this process, we must use a scaled subtraction in order to adjust the intensities of them. The scale factor is determined from the calculation of the least residuals.

The most important thing in the image processing is the matching of disks. In the matching of two images, we calculate the displacement between them by

$$r(k,l) = \Sigma(A(x,y) - B(x+k, y+l))^2$$

We shift the image B to the image A pixel by pixel and find the displacement (k,l) with the least r. We think that the matching have an accuracy of $\sim$1 pixel.

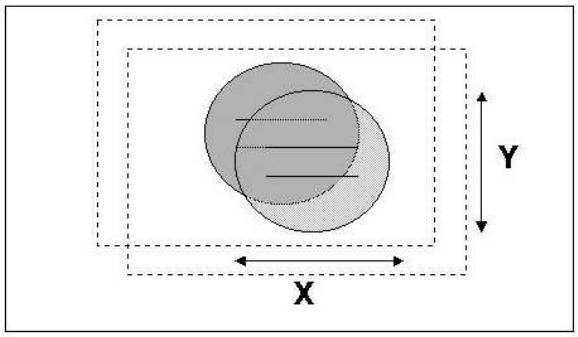

Figure 24: Schematic diagram of the matching.

5 Results and Discussion

5.1 Results

We obtained the data in a good condition of Earth's atmosphere in the period from October 29 to November 1, 2001. In this section, we show the results of the data obtained by the FWHM 1.55 nm filter on November 1 st. Since the CML was $\sim 160^{\circ}$ at the time of observation, we obtained Hα and BG images of Jupiter's northern auroral region. We obtained 100 frames of Hα and BG images with exposure times of 200 ms, and 200 frames with 100 ms. The results of image processing are shown in Fig 25, 26, 27, 28, and 29. The exposure time and the number of frames are shown in figures. In each figure, the top, middle and bottom panels show the Hα images, the BG images, and the subtracted images respectively. In each panel, North is top and West is to the right. The left panels show the profiles of intensity through the center of the discs from north to south.

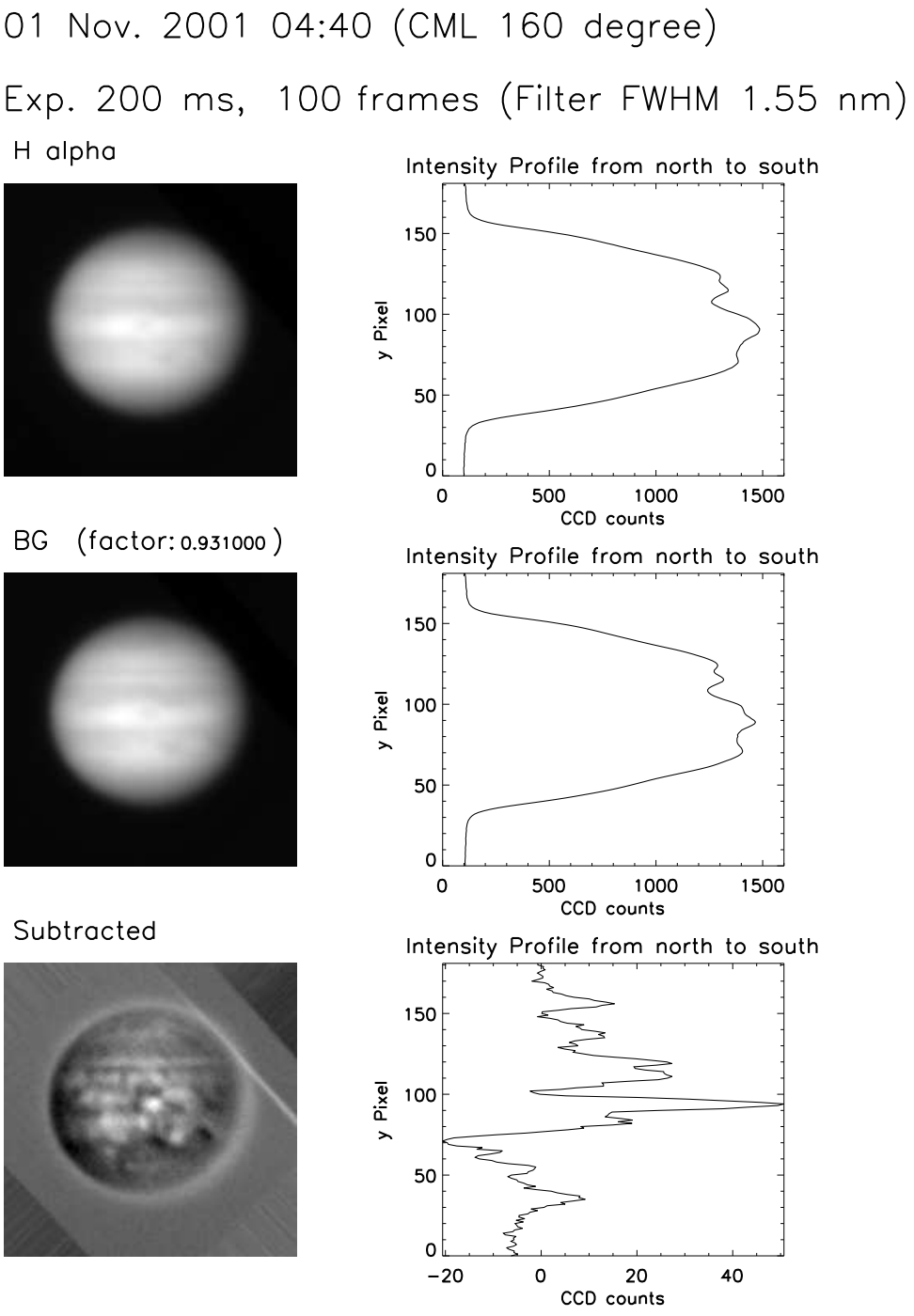

Figure 25: Result of 100 frames with an exposure time of 200 ms. The top, middle and bottom panels show the Hα image, the BG image, and the subtracted image respectively. In each panel, North is top and West is to the right. The left panels show the profiles of the intensity from north to south.

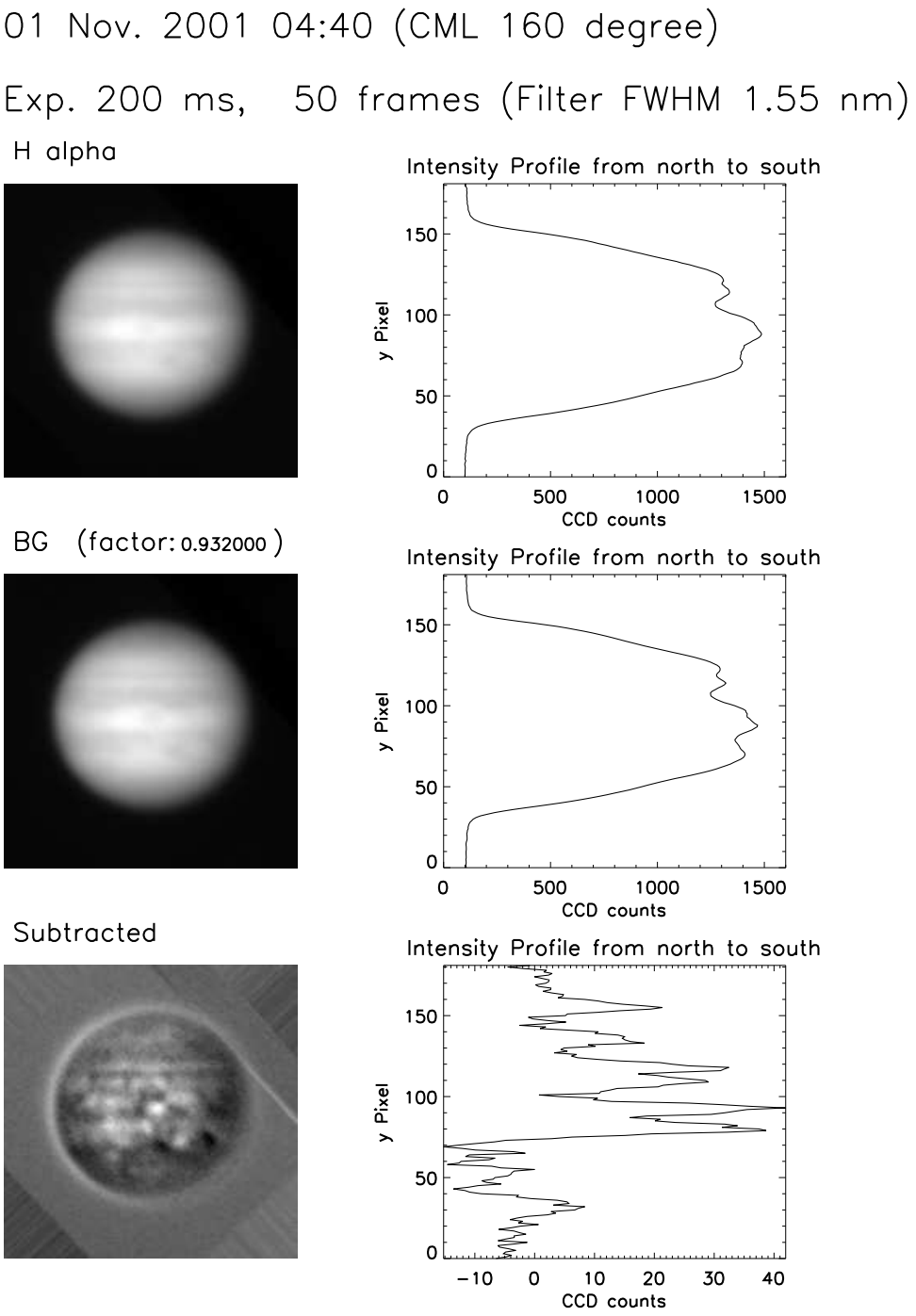

Figure 26: Result of 50 frames with an exposure time of 200 ms.

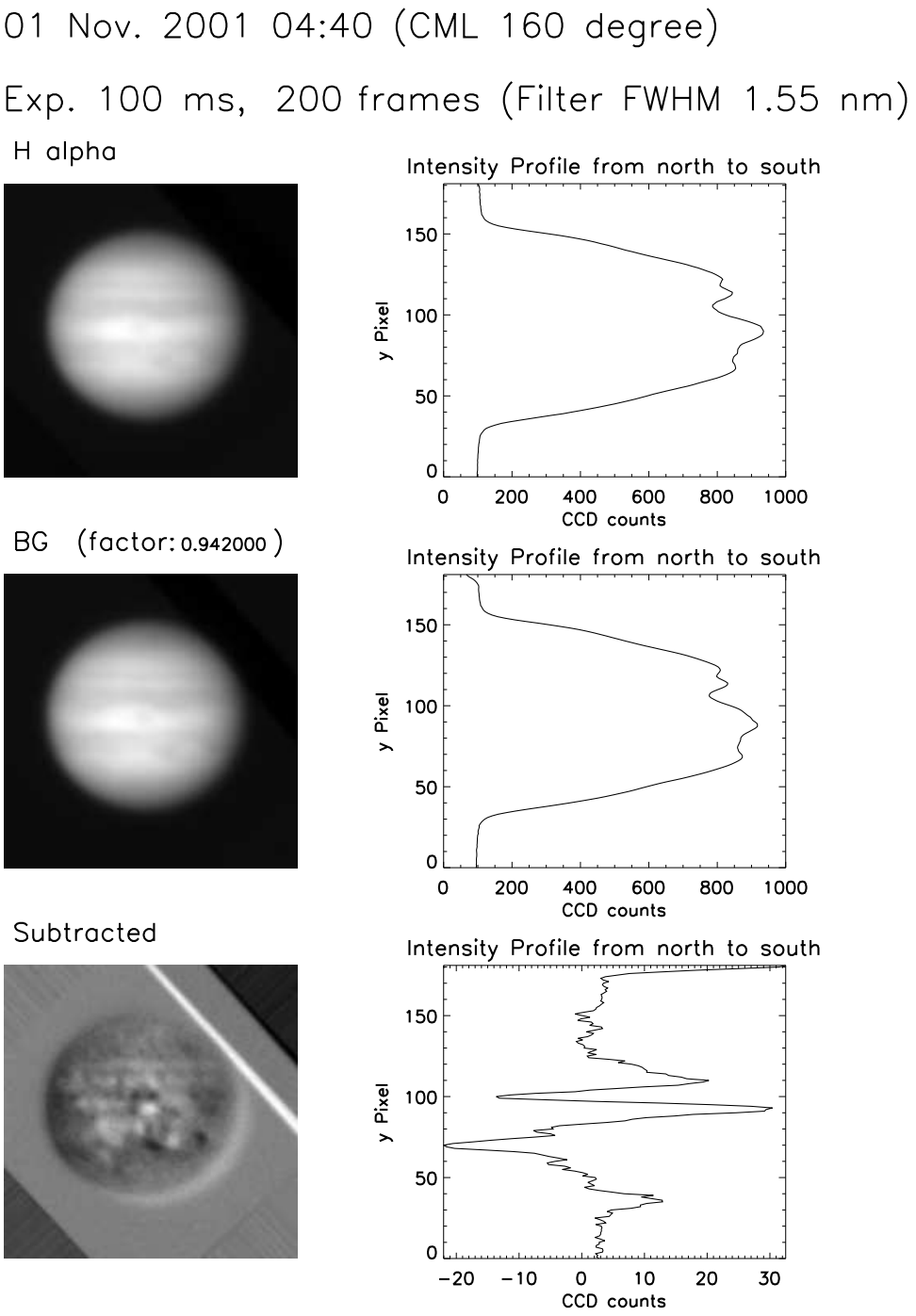

Figure 27: Result of 200 frames with an exposure time of 100 ms.

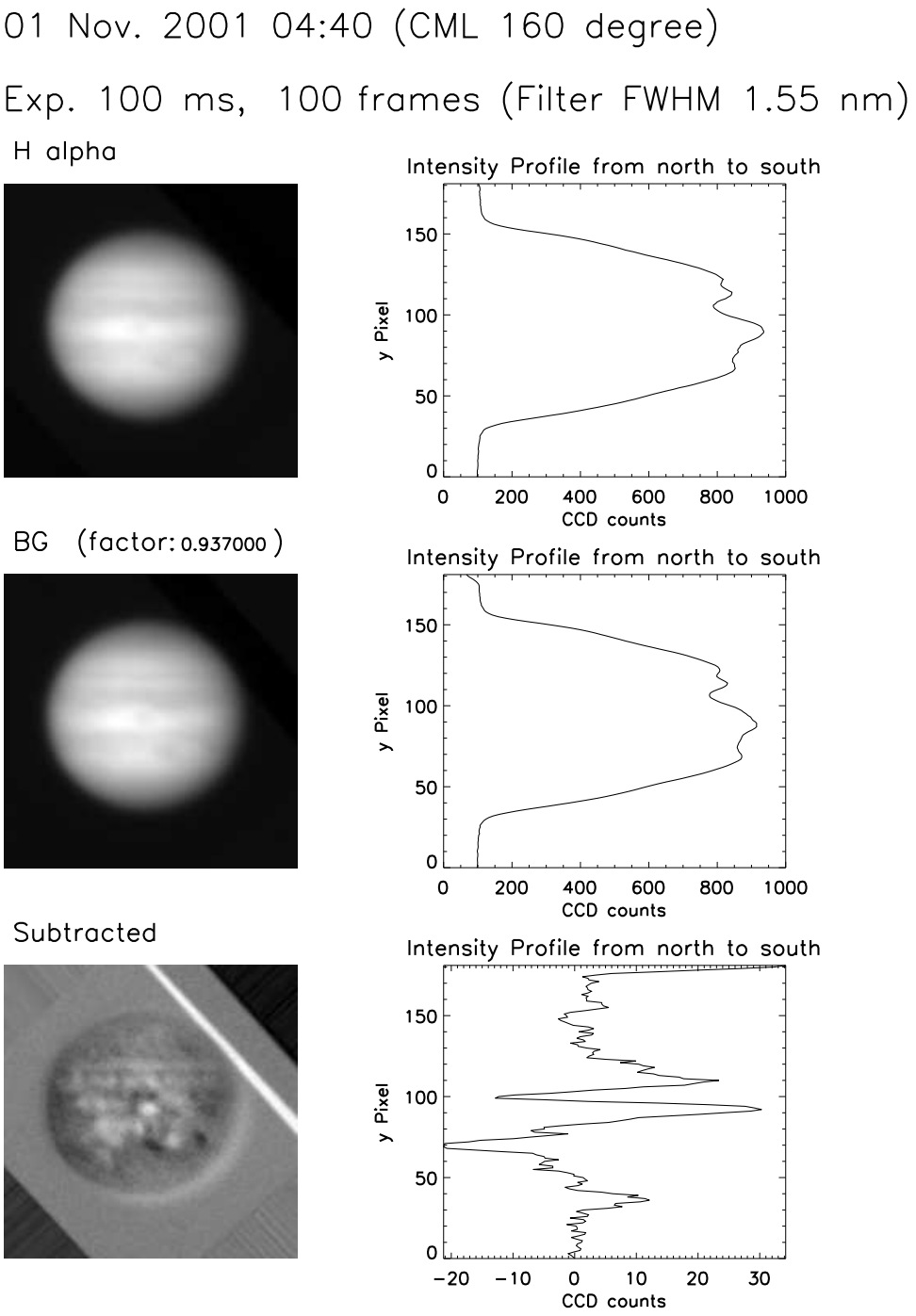

Figure 28: Result of 100 frames with an exposure time of 100 ms.

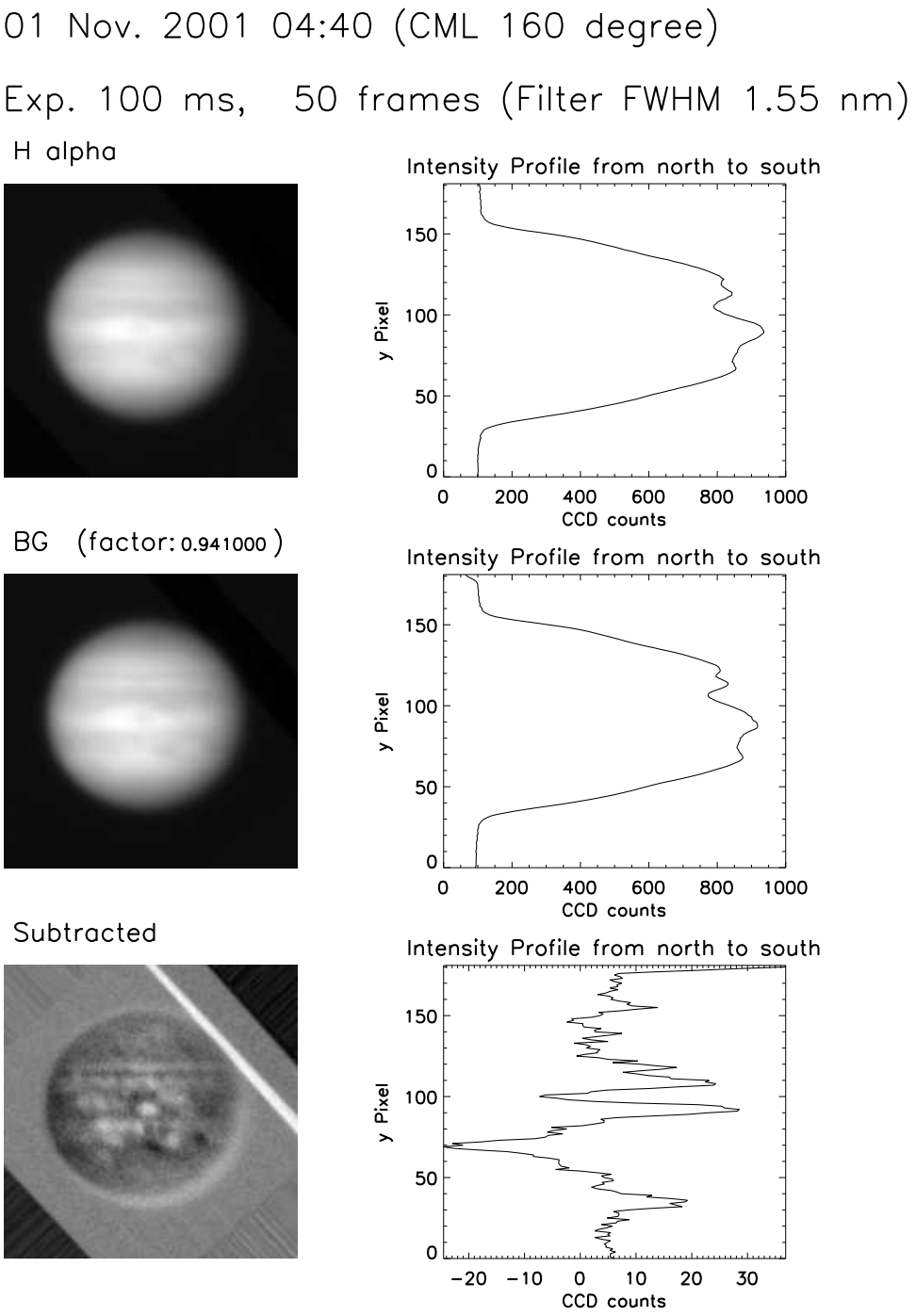

Figure 29: Result of 50 frames with an exposure time of 100 ms.

5.2 Discussion

We detected some Hα emissions in subtracted images obtained by image processing of 200 ms frames. Fig 30 shows the subtracted image and the profile of intensity in Fig 25. The range of Hα emissions from peak to peak in the subtracted image is $\sim$70 counts. And the maximum intensity in the composite images is $\sim$1400 counts. Therefore, the S/N ratio in this image processing is $\sim$5 %. In other words, this image processing can detect signals with more than 5 % S/N ratios.

In Jupiter's northern auroral region in the subtracted image, there is a faint emission which would be due to a auroral emission. The intensity of the faint emission is $\sim$10 counts (Fig 30). The intensity of the background emission in northern auroral region in the composite Hα image is roughly 800 counts (Fig 25). Therefore, the ratio of the faint emission to background intensity is about $\sim$1.3 %. These results were obtained in the image processing of 100 frames with 200 ms. Additionally, in a 200 ms Hα image before composition, the intensity of Jupiter's disk is $\sim$36000 counts. The fluctuation of the composite image is $\sim \pm\sqrt{36000}/100$ counts. Therefore, we think that the range of error in this image processing is $\sim$4 counts.

The spatial distribution of the faint emission is, however, broad in several pixels in comparison with the actual distribution of the auroral oval (Fig 31). Since the limiting resolution of ground-based observation is $\sim$1 ", the distribution of the auroral oval would be diffused over several pixels in our observation. Therefore, the actual intensity of the auroral emission would be several times brighter than the intensity in the image. If we consider this factor, the S/N ratio which I mentioned above might correspond to $\sim$5 %. This $\sim$5 % is, however, smaller than the S/N ratio which we estimated when we take into account a composition process in image processing.

In our conclusion, the actual intensity of the Jupiter's visible aurora might be a little weaker than the intensity from previous researches.

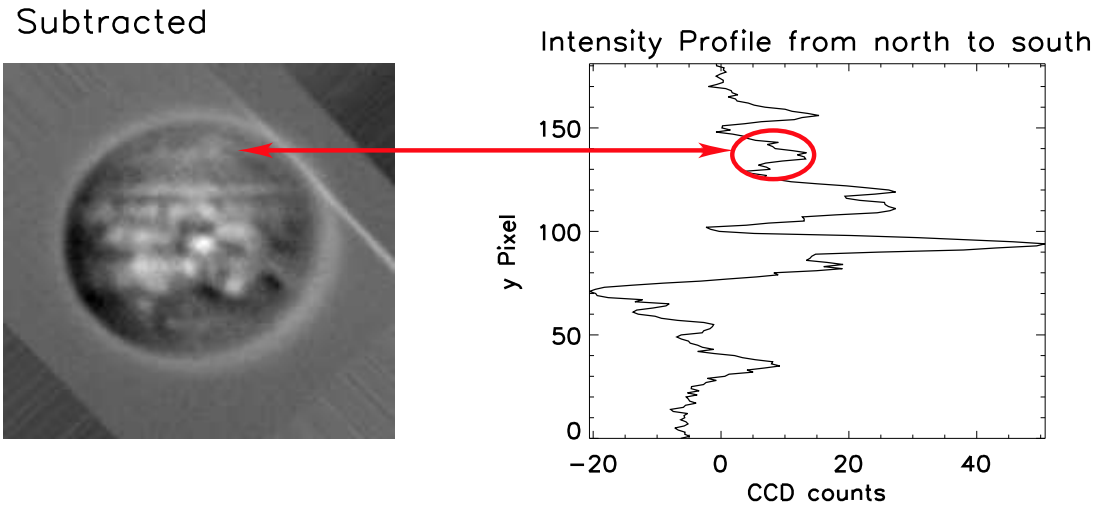

Figure 30: The subtracted image and the profile of intensity shown in Fig 25. The intensity of the faint emission is $\sim$10 counts.

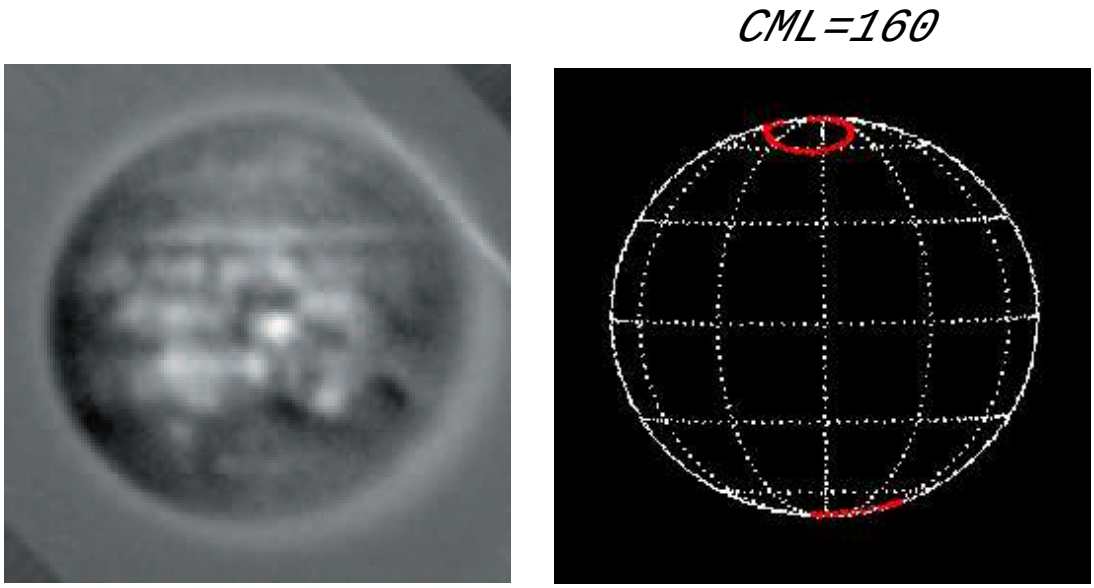

Figure 31: The left panel shows the subtracted image shown in Fig 25, and the right panel shows the distribution of the actual auroral oval illustrated in red line at CML = 160°.

6 Summary

We observed Jupiter by using 115-cm telescope at Ginganomori Observatory, Hokkaido, and 60-cm telescope at the Iitate Observatory, Fukushima in Japan from November 1999 to November 2001. We analyzed the data acquired on October 29 - November 1. We detected a faint emission at Hα wavelength in Jupiter's northern auroral region the image processing of 100 frames with 200 ms. The ratio of the faint emission to background intensity is about $\sim$1.3 %.

Future works to understand more details about the emission will be:

1. To improve the Imaging processing. We will improve the Imaging processing by selecting good seeing images in the composition.

2. To analyze more data set
   We will analyze date obtained at other time, and compare results of them in order to find the variations in intensity and distribution.

Our technique may be applied to other observations such as faint emissions on planetary atmosphere and faint luminous bodies.

Acknowledgments

I would like to express my special thanks to Professor Shigeto Watanabe for giving me an opportunity to engage such an interesting study. I would like to mention my sincere thanks to Dr. Yukihiro Takahashi who is a lecture at Tohoku University. Through this study, Dr. Takahashi gave me a lot of advice not only on my research but also on my life. I also express my sincere appreciation to Associate Prof. Kiyoshi Kuramoto for his guidance and encouragement during my master course. I also thank Mr. Hiromasa Nozawa for his advised about the image processing. I also thank Mr. Atsushi Ohkubo for his help in observation and all members of Planetary Atmosphere physics laboratory at Tohoku University. I express my thanks to all members of our laboratory for help and encouragement through my master course. Finally, I want to express my deep thanks to my family for supporting me with their love.

Reference

- Baron, R. L., T. Owen, J. E. P. Connerney, T. Sato, and J. Jarrington, 1996, Solar Wind Control of Jupiter's H_3^+ Aurora, *Icarus, 120*, 437-442.
- Bhardwaj, A., and G. R. Gladston, 2000, Auroral emission of the giant planets, *Reviews of Geophyscs, 38*, 295-354.
- Clary, R. S. and J. H. Hunter, 1975, Hydrogen-alpha auroral activity on Jupiter, *Astrophys. J., 199*, 517-529.
- Cook, A. F., A. V. Jones, and D. E. Shemansky, 1981, visibe Aurora in Jupiter's Atmosphere?, *J. Geophys. Res., 86*, 8793-8796.
- Drossart, P., J.-P. Maillard, J. Caldwell, S. J. Kim, J. K. G. watson, W. A. Majewski, J.Tennyson, S. Miller, S. K. Atreya, J. T. Clarke, J. H. Waite, and R. Wagener, 1989, Detection of H_3^+ on Jupiter, *Nature, 340*, 539-541.
- Holman, B. L. and J. H. Hunter, 1977, Hydrogen-alpha auroral activity on Jupiter. II., *Astrophys. J., 213*, 906-907.
- Hunter, J. H., 1969, Hα Auroral Activity on Jupiter, *Nature, 223*, 338-389.
- Ingersoll, A. P., A. R. Vasavada, B. Little, C. D. Anger, S. J. Bolton, C. Alexander, K. P. Klaasen, W. K. Tobiska, and the Galileo SSI Team, 1998, Imaging Jupiter's Aurora at Visible Wavelengths, *Icarus, 135*, 251-264.
- Mai, H and K. Jockers, 2000, Fabry-Perot Imaging of Jupiter's Aurora at 2.1 μm, *Icarus, 146*, 494-500.
- Sato, T., J. E. P. connerney, 1999, Jupiter's H_3^+ Emissions Viewd in Corrected Jovimagnetic Coordinates, *Icarus 141*, 236-252.
- Vasavada, A. R., A. H. Bouchez, A. P. Ingersoll, B. Little, C. D. Anger, and the Galileo SSI Team, 1999, Jupiter's visibe aurora and Io footprint, *J. Geophys. Res., 104*, 27,133-27,142.
- Waite, J. H., G. R. Gladstone, W. S. Lewis, R. Goldstein, D. J. McComas, P. Riley, R. J. Walker, P. Robertson, S. Desai, J. T. Clarke, and D. T. Young, 2001, An auroral flare at Jupiter, *Nature, 410*, 787-789.